



Comprehensive Analysis of the Open Cluster Collinder 74

T. Yontan^{1*} , and R. Canbay² 

¹Istanbul University, Faculty of Science, Department of Astronomy and Space Sciences, 34119, Beyazit, Istanbul, Turkiye

²Istanbul University, Institute of Graduate Studies in Science, Programme of Astronomy and Space Sciences, 34116, Beyazit, Istanbul, Turkiye

ABSTRACT

In this study, we have used the *Gaia* Third Data Release (*Gaia* DR3) to investigate an intermediate-age open cluster Collinder 74. We have identified 102 probable cluster members by considering stars with a membership probability exceeding 0.5 and located within the designated confinement radius. The mean proper-motion components of Collinder 74 are estimated as $(\mu_\alpha \cos \delta, \mu_\delta) = (0.960 \pm 0.005, -1.526 \pm 0.004)$ mas yr⁻¹. We detected previously confirmed four blue straggler stars which show flat radial distribution. Colour excess, distance, and age of the cluster were estimated simultaneously by fitting PARSEC isochrones to the observational data on *Gaia* based colour magnitude diagram. These values were derived as $E(G_{BP} - G_{RP}) = 0.425 \pm 0.046$ mag, $d = 2831 \pm 118$ pc and $t = 1800 \pm 200$ Myr, respectively. The mass function slope was estimated as $\Gamma = 1.34 \pm 0.21$ within the mass range $0.65 \leq M/M_\odot \leq 1.58$ which is well matched with that of Salpeter. Stellar mass distribution indicated that the massive and most likely stars are concentrated around the cluster center. The total mass of the cluster was found to be $365 M/M_\odot$ for the stars with probabilities $P > 0$. Galactic orbit integration shows that the Collinder 74 follows a boxy pattern outside the solar circle and is a member of the thin-disc component of the Galaxy.

Keywords: Galaxy: open clusters and associations; individual: Collinder 74; stars: Hertzsprung Russell (HR) diagram; Galaxy: Stellar kinematics

1. INTRODUCTION

Open star clusters (OCs), also known as Galactic clusters, are loosely bound groups of stars that emerged from the same molecular cloud, sharing a common origin and age. As relatively young and dynamically active systems, OCs typically contain hundreds to thousands of stars that share similar chemical composition, age, and distance. The formation origin of OCs plays a crucial role in our understanding of stellar formation and evolution and makes them ideal laboratories for studying stellar properties, such as temperature, luminosity, and mass (Lada & Lada 2003; Kim et al. 2017). Also, member stars of OCs have similar movement directions in the sky, this knowledge makes proper-motion components useful tools for separating physical members from the field star contamination (Sariya et al. 2021). This method provides a reliable sample of member stars for the estimation of astrophysical parameters for OCs (Bisht et al. 2020; Sariya et al. 2021).

In this study, we estimated the structural, kinematic, and astrophysical properties of Collinder 74 (Coll 74) open cluster. The cluster is positioned at $\alpha = 05^h48^m40^s.8$, $\delta = +07^\circ22'26''.4$ (J2000) corresponding to Galactic coordinates $l = 199^\circ.019$, $b = -10^\circ.379$ according to Cantat-Gaudin et al. (2020). Coll 74 is a centrally concentrated old open cluster

located in the third Galactic quadrant toward the Galactic anti-center region. Ann et al. (1999) afforded *UBVI* CCD photometry and suggested that the age of the cluster is 1300 ± 200 Myr and it is located at 2511 ± 245 pc from the Sun. Tadross (2001) performed *UBV* CCD observations and defined colour excess, distance and age of the cluster as $E(B - V) = 0.38$ mag, $d = 2254$ pc and $t = 1600$ Myr, respectively. Dias et al. (2006) presented the kinematics of the cluster using UCAC2 Catalogue positions and proper motions. They derived proper-motion components as $(\mu_\alpha \cos \delta, \mu_\delta) = (-0.49, -3.49)$ mas yr⁻¹. Carraro & Costa (2007) investigated CCD photometry in the *V* and *I*-bands and obtained colour excess, distance and age of the cluster as $E(B - V) = 0.28 \pm 0.04$ mag, $d = 1500$ pc and $t = 3000$ Myr, respectively. From the analyses of *BVI* photometry Hasegawa et al. (2008) concluded that the Coll 74 is 3680 pc away from the Sun and 1400 Myr old cluster. Dias et al. (2014) derived the mean proper-motion components by taking into account the U.S. Naval Observatory CCD Astrograph Catalogue (UCAC4; Zacharias et al. 2013) as $(\mu_\alpha \cos \delta, \mu_\delta) = (1.92 \pm 0.55, -3.00 \pm 0.10)$ mas yr⁻¹. Loktin & Popova (2017) redetermined main parameters using published photometric measurements provided by 2MASS catalogue for 959 clusters including Coll 74. They estimated colour excess, distance and age as $E(B - V) = 0.418$

Corresponding Author: T. Yontan E-mail: talar.yontan@istanbul.edu.tr

Submitted: 29.09.2023 • Revision Requested: 18.10.2023 • Last Revision Received: 19.10.2023 • Accepted: 20.10.2023



This article is licensed under a Creative Commons Attribution-NonCommercial 4.0 International License (CC BY-NC 4.0)

Table 1. Basic parameters of the Collinder 74 open cluster collected from the literature.

$E(B - V)$ (mag)	μ_V (mag)	d (pc)	[Fe/H] (dex)	t (Myr)	$\langle \mu_\alpha \cos \delta \rangle$ (mas yr ⁻¹)	$\langle \mu_\delta \rangle$ (mas yr ⁻¹)	V_γ (km s ⁻¹)	Ref
0.38±0.04	13.08±0.25	2511±245	0.07	1300±200	–	–	–	(01)
0.38	13.00	2254	0.054	1600	–	–	–	(02)
0.38	13.21	2549	–	1300	–	–	–	(03)
–	–	–	–	–	-0.49	-3.49	–	(04)
0.28±0.04	11.75±0.10	1500	–	3000	–	–	–	(05)
0.36	13.95	3680	-0.38	1400	–	–	–	(06)
0.604	13.98	2637	–	1230	0.91	-3.86	–	(07)
–	–	–	–	–	1.92±0.55	-3.00±0.10	–	(08)
–	–	2510	0.050	1288	–	–	–	(09)
0.418	12.588	3293	–	1400	0.294±0.181	-1.091±0.172	–	(10)
–	–	–	–	–	0.77±2.15	0.47±3.54	–	(11)
–	–	2453 ⁺⁷⁹⁷ ₋₄₈₄	–	–	1.011±0.016	-1.512±0.016	–	(12)
–	–	2453 ⁺⁷⁹⁷ ₋₄₈₄	–	–	1.011±0.016	-1.512±0.016	20.18±0.39	(13)
–	–	2747±332	–	2190±131	0.981±0.200	-1.497±0.199	–	(14)
–	–	2453 ⁺⁷⁹⁷ ₋₄₈₄	-0.05±0.03	–	1.011±0.121	-1.512±0.122	15.94±17.57	(15)
0.274	11.99	2498±494	–	1900	1.011±0.121	-1.512±0.122	–	(16)
0.391±0.076	–	2153±144	-0.083±0.084	2760	0.995±0.170	-1.528±0.175	20.20±0.80	(17)
–	–	2356	–	2100	1.011±0.121	-1.512±0.122	20.18±0.39	(18)
0.511±0.074	–	2466±22	–	627±348	0.964±0.007	-1.546±0.007	20.93±4.10	(19)
0.301±0.033	13.052±0.088	2831±118	0.052±0.034	1800±200	0.960±0.005	-1.526±0.004	20.55±0.41	(20)

(01) Ann et al. (1999), (02) Tadross (2001), (03) Lata et al. (2002), (04) Dias et al. (2006), (05) Carraro & Costa (2007), (06) Hasegawa et al. (2008), (07) Kharchenko et al. (2013), (08) Dias et al. (2014), (09) Marsakov et al. (2016), (10) Loktin & Popova (2017), (11) Dias et al. (2018), (12) Cantat-Gaudin et al. (2018), (13) Soubiran et al. (2018), (14) Liu & Pang (2019), (15) Zhong et al. (2020), (16) Cantat-Gaudin et al. (2020), (17) Dias et al. (2021), (18) Tarricq et al. (2021), (19) Hunt & Reffert (2023), (20) This study

mag, $d = 3293$ pc and $t = 1400$ Myr, respectively. Also, from RAVE catalogue Loktin & Popova (2017) estimated proper-motion components in equatorial coordinate system as $(\mu_\alpha \cos \delta, \mu_\delta) = (0.294 \pm 0.181, -1.091 \pm 0.172)$ mas yr⁻¹, respectively.

With the first data release of the *Gaia* (Gaia Collaboration et al. 2016), many researchers investigated the astrometric and kinematic properties of the Coll 74. According to literature studies performed with *Gaia* data, values of the mean radial velocity of the cluster differs from 15.94 ± 17.57 km s⁻¹ (Zhong et al. 2020) to 20.20 ± 0.80 km s⁻¹ (Dias et al. 2021) and distance to the Sun changes between 1500 pc (Carraro & Costa 2007) and 3680 pc (Hasegawa et al. 2008). Also, the age of the cluster varies from 1230 Myr (Kharchenko et al. 2013) to 3000 Myr (Carraro & Costa 2007). The literature results are listed in Table 1 for detailed comparison. The main purpose of this study is to find out structural, astrophysical, and kinematic properties of the Coll 74 open cluster.

2. DATA

The astrometric, photometric, and spectroscopic data for Coll 74 open cluster was taken from *Gaia*'s third data release (*Gaia* DR3, Gaia Collaboration et al. 2023). To do this, we used the central equatorial coordinates of Cantat-Gaudin et al. (2020) $\langle \alpha, \delta \rangle = (05^h 48^m 40^s .8, +07^\circ 22' 26'' .4)$ and compiled the detected stars in the direction of the cluster for $35'$ -radius field. Hence, we identified 73,326 stars within the applied radius. The

finding chart of the Coll 74 ($35' \times 35'$) is shown in Figure 1. The main cluster catalogue contains each stars' position (α, δ), photometric magnitude and colour index ($G, G_{BP} - G_{RP}$), trigonometric parallax (ϖ), proper-motion components ($\mu_\alpha \cos \delta, \mu_\delta$), radial velocity (V_γ) and their errors within the $8 < G \leq 22$ mag.

To achieve reliable structural and astrophysical parameters for Coll 74, we obtained a faint limited magnitude of the used data. For this, we calculated the number of stars that correspond to the G magnitude intervals. The histogram of a number of stars versus G magnitudes is shown in Figure 2, where a number of stars rise towards the fainter G magnitudes and declines after a certain limit. This limit value is $G = 20.5$ mag for the Coll 74 and in the following analyses, we used only the stars brighter than $G = 20.5$ mag. We calculated the mean photometric errors of the stars for G magnitude intervals. The mean errors for G and $G_{BP} - G_{RP}$ colour indices reach up 0.011 and 0.228 mag for $G = 20.5$ limiting magnitude, respectively. The photometric errors for G magnitudes and $G_{BP} - G_{RP}$ colour indices versus G magnitude intervals are shown in Figure 3.

3. RESULTS

3.1. Spatial structure of Collinder 74

To interpret stellar distribution within the cluster we constructed the radial density profile (RDP) considering adopted central equatorial coordinates presented by Cantat-Gaudin et al. (2020). We divided the $35'$ cluster region into many concentric rings surrounding the cluster center and calculated stellar

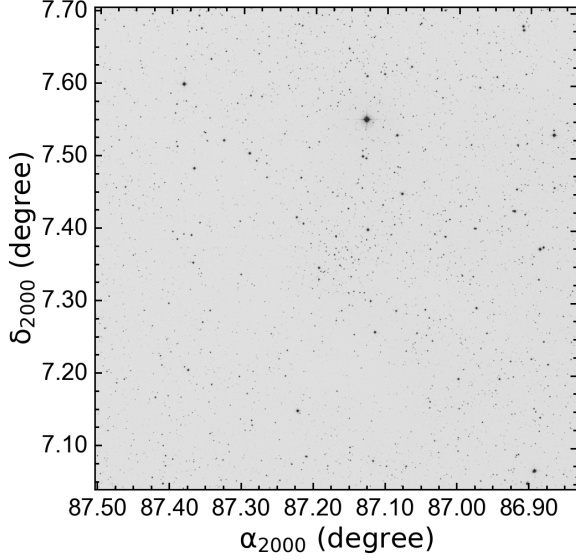


Figure 1. Finding chart of the Coll 74 for $35' \times 35'$ region. Up and left directions represent North and East, respectively.

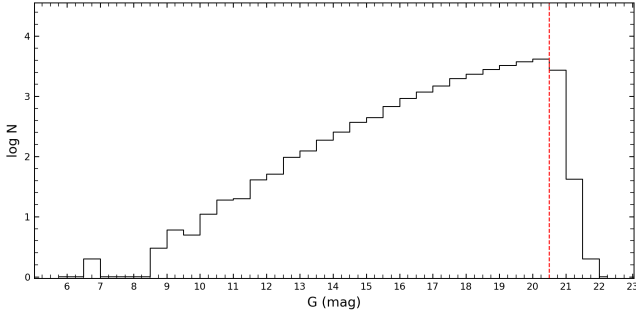


Figure 2. Distribution of the stars in the direction of Coll 74 for G magnitude intervals. The photometric completeness limit is indicated by a red dashed line.

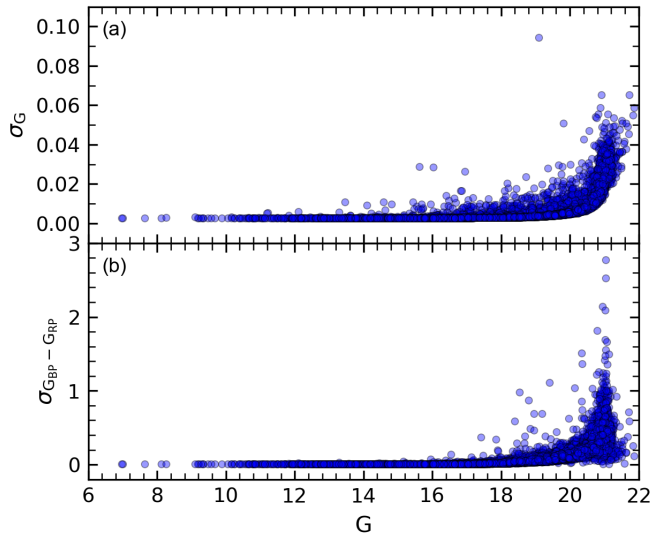


Figure 3. Distribution of mean photometric errors obtained for G apparent magnitude (a) and $G_{BP} - G_{RP}$ colour index versus G magnitude intervals.

densities ($\rho(r)$) from the stars within $G \leq 20.5$ mag. The stellar densities in i^{th} ring were calculated by the equation of

$R_i = N_i/A_i$, where, N_i and A_i indicate the number of stars and area of related ring, respectively. To visualise RDP, we plotted stellar density distribution versus distance from cluster center and fitted the empirical King (1962) model identified by the following equation:

$$\rho(r) = f_{bg} + \frac{f_0}{1 + (r/r_c)^2}. \quad (1)$$

Here, r is the radius of the cluster. The f_{bg} , f_0 , r_c are the background stellar density, the central stellar density and the core radius, respectively. We used the minimum χ^2 estimation for RDP analyses and estimated f_{bg} , f_0 and r_c . In Figure 4 we showed the best-fit result of RDP which is demonstrated by the black solid line. It can be seen from the figure that stellar density is higher near the cluster center and it flattens toward the outer region of the cluster and at a point merges with the field star density. This point is described as limiting radius (r_{lim}) and visually adopted as $10'$. The best-fit solution of RDP analyses resulted that the structural parameters to be $f_0 = 8.42 \pm 0.35$ stars arcmin $^{-2}$, $f_{bg} = 5.45 \pm 0.16$ stars arcmin $^{-2}$ and $r_c = 1.38 \pm 0.12$ arcmin for the Coll 74.

3.2. Membership Analyses of Collinder 74

Working with a sample of stars that are part of the cluster itself is crucial to accurately characterise its properties, such as its age, mass, luminosity function, and dynamics. Field star contamination may contribute to noise and bias during the analyses and can cause inaccurate results. Therefore, field star separation is necessary to understand the astrophysical, astrometric, and kinematic properties of the studied cluster. As their physical formation processes, cluster members are gravitationally

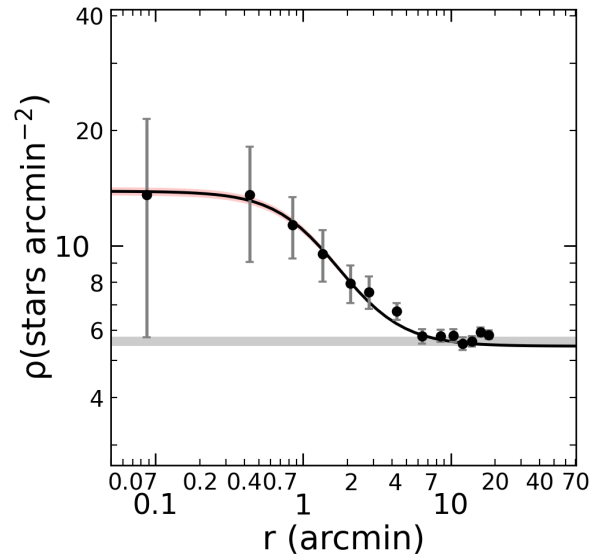


Figure 4. The RDP of King (1962) for Coll 74. Stellar density errors were determined from Poisson statistics $1/\sqrt{N}$, where N is the number of stars. The fitted black curve and horizontal grey shaded area show the best-fitted RDP and background stellar density, respectively. Also, red-shaded area indicates the 1σ uncertainty of the fit.

bound to the cluster. Therefore, they exhibit similar vectorial movements across the sky relative to the background field stars. By analyzing proper-motion components, it becomes possible to identify stars that share the cluster's motion characteristics as potential cluster members. Hence, proper-motion components are useful tools to separate cluster members and calculate their membership probabilities (Sariya et al. 2021; Bisht et al. 2020). The precise astrometric data from *Gaia* DR3 data (Gaia Collaboration et al. 2023) provide a crucial role for membership analyses.

We used the method of Photometric Membership Assignment in Stellar Clusters (UPMASK, Krone-Martins & Moitinho 2014) considering *Gaia* DR3 astrometric data to calculate membership probabilities of stars in the region of the Coll 74. UPMASK uses a clustering algorithm to group stars that have similar positions, proper-motion components, trigonometric parallaxes and are close to each other in space. The algorithm then assigns membership probabilities to each star based on its likelihood of belonging to a particular cluster. We utilised the method in five-dimensional astrometric space considering astrometric measurements (α , δ , $\mu_\alpha \cos \delta$, μ_δ , ϖ), also their uncertainties, of each star. To determine the membership possibilities (P) of stars we run the program with 100 iterations. As a result, taking into account the stars within both the estimated limiting radius ($r_{\text{lim}}=10'$) and the completeness limit $G = 20.5$ mag, for the open cluster Coll 74 we obtained 102 most likely member stars with membership probabilities of $P \geq 0.5$. These stars are used in the estimation of astrometric and astrophysical parameters of Coll 74.

To visualise the clustering of the most likely member stars, we plotted vector-point diagram (VPD) by using proper-motion components of the stars and showed it in Figure 5. It is evident from the VPD that Coll 74 is embedded in the field stars. Even if this is the case, the cluster structure can be distinguished by investigating the probability values of the stars. We estimated mean proper-motion values from the stars with membership probabilities greater than 0.5 and found the values as $(\mu_\alpha \cos \delta, \mu_\delta) = (0.960 \pm 0.005, -1.526 \pm 0.004)$ mas yr $^{-1}$. The trigonometric parallax histogram of the most likely member stars is shown in Figure 6. By fitting the Gaussian function to the histogram, we estimated the mean trigonometric parallax as $\varpi = 0.363 \pm 0.043$ mas for the Coll 74 and corresponding distance value (with the linear equation $d(\text{pc}) = 1000/\varpi$) mas as $d_\varpi = 2755 \pm 326$ pc. This distance value is close to the values estimated in *Gaia* era, as listed in Table 1.

3.3. The Blue Straggler Stars of Collinder 74

Blue straggler stars (BSSs) in open clusters defy the natural aging process by appearing younger and bluer than their surrounding companions. While most stars in open clusters follow common evolutionary processes, BSSs defy the laws of stellar evolution in the cluster by reversing this trend. Interactions

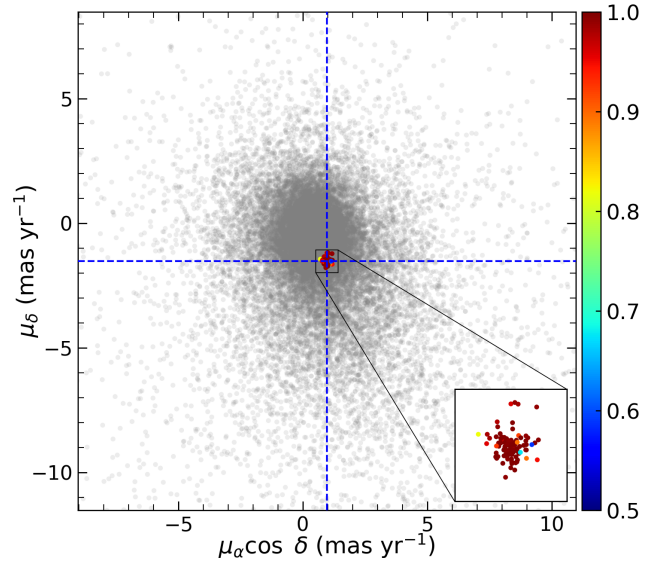


Figure 5. VPD of Coll 74. The colour scale on the right panel indicates the membership probabilities of the stars for the cluster. The enlarged panel inset shows the cluster's denser region in VPD. The intersection of the dashed blue lines represents the mean proper-motion value for Coll 74.

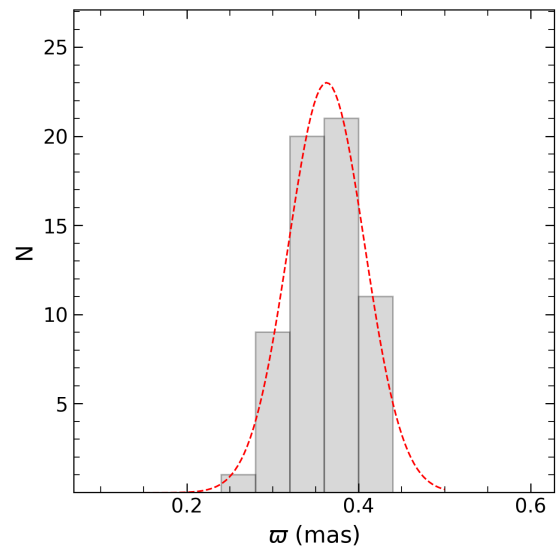


Figure 6. Histogram of star count of the most likely members ($P \geq 0.5$) in trigonometric parallaxes. The red dashed line indicates the fitted Gaussian function.

between stars in binary systems or stellar collisions within the dense cluster environment are among the leading formation mechanisms for BSSs (Sandage 1953; Zinn & Dahn 1976; Hills & Day 1976).

We identified four BSSs in Coll 74. These stars are confirmed as cluster members with membership probabilities $P \geq 0.9$. The positions of BSSs are shown in Figure 7. Rain et al. (2021) defined five BSSs by using *Gaia* DR2 (Gaia Collaboration et al. 2018) photometric and astrometric data. Due to the membership analyses being based on *Gaia* DR3 data and we took into account the stars within limiting radius ($r_{\text{lim}} \leq 10'$),

one of the Rain et al. (2021) BSS was not considered. Jadhav & Subramaniam (2021) using *Gaia* DR2 data and identified BSSs in 1246 open clusters. They found four BSSs members in Coll 74 which are the same star sample as presented in this study.

Ferraro et al. (2012) considering the radial distribution of BSSs in the clusters, defined three classes for BSSs. Three of BSSs in Coll 74 are located at a radial distances of 0.42, 0.88, and 0.98 arcmin, whereas one star is located at 6.25 arcmin. According to their radial distribution and the criterion of Ferraro et al. (2012), we can conclude that the BSSs of Coll 74 show flat distribution and cluster belongs to the family I. The formation mechanisms of blue stragglers in family I clusters are thought dominantly to be caused by stellar collisions and mass transfer in close binary systems.

3.4. Astrophysical Parameters of Collinder 74

To derive age, distance modulus and colour excess of Coll 74, we fitted theoretical PARSEC isochrones of Bressan et al. (2012) to the observed CMD constructed from the most likely cluster members. The age, distance modulus and colour excess of the cluster were estimated simultaneously, while the metallicity of Coll 74 was taken from Zhong et al. (2020) as $[\text{Fe}/\text{H}] = -0.052 \pm 0.034$ dex. We fitted PARSEC models by taking into account the morphology of the cluster and reached the best fit. For the selection of the isochrones and estimation of astrophysical parameters, we transformed the assumed metallicity ($[\text{Fe}/\text{H}] = -0.052 \pm 0.034$ dex) to the mass fraction z . To do this, we applied the equation of Bovy¹ that are available for PARSEC models (Bressan et al. 2012). The equations are given as follows:

$$z_x = 10^{[\text{Fe}/\text{H}] + \log\left(\frac{z_\odot}{1 - 0.248 - 2.78 \times z_\odot}\right)}, \quad (2)$$

and

$$z = \frac{(z_x - 0.2485 \times z_x)}{(2.78 \times z_x + 1)}. \quad (3)$$

where z_x and z_\odot are intermediate values where solar metallicity z_\odot was adopted as 0.0152 (Bressan et al. 2012). The calculated mass fraction is $z = 0.0136$ for Coll 74.

We plotted $G \times (G_{\text{BP}} - G_{\text{RP}})$ and superimposed isochrones, scaled to the $z = 0.0136$, of different ages ($\log t = 9.20, 9.25$ and 9.30 yr) by visual inspection to the most likely cluster main-sequence, turn-off and giant members with probabilities over $P \geq 0.5$ as shown in Figure 7. The best fit supports the isochrone with $\log t = 9.25$ yr to the cluster morphology, this isochrone corresponding to $t = 1800 \pm 200$ Myr. The estimated age is comparable with the values of Tadross (2001) and Cantat-Gaudin et al. (2020). Also, good isochrone fitting result supplies the distance modulus and colour excess of the Coll 74

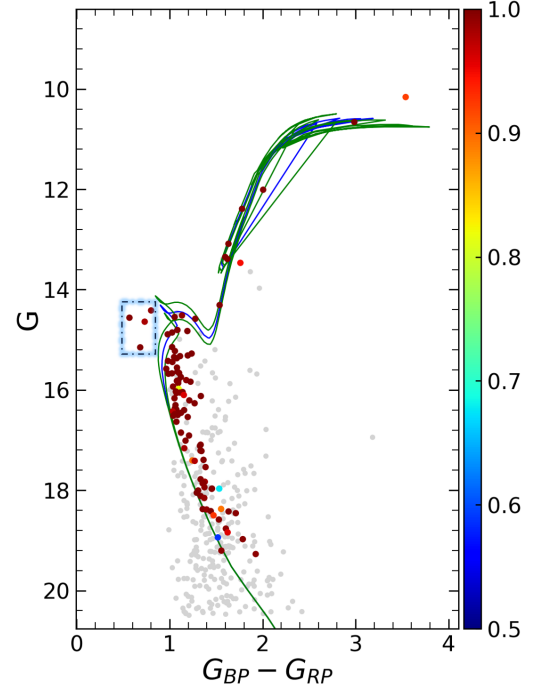


Figure 7. Colour-magnitude diagram for the studied cluster Coll 74. Different colour and colourbar scales show the membership probabilities of stars with $P \geq 0.5$. Stars with probabilities $P < 0.5$ are demonstrated with filled grey circles. BSSs of the cluster are shown in a blue dashed-lined box. The best solution of fitted isochrones and their errors are inferred as the blue and green lines, respectively. The age of the blue-lined isochrone matches 1800 Myr for the cluster.

to be $\mu_G = 13.052 \pm 0.088$ mag, corresponding to isochrone distance $d_{\text{iso}} = 2831 \pm 118$ pc and $E(G_{\text{BP}} - G_{\text{RP}}) = 0.425 \pm 0.046$ mag, respectively. We used the relations of Carraro et al. (2017) to estimate the errors of distance modulus and isochrone distance. Our derived isochrone distance is compatible with most of the studies presented by different researchers (see Table 1) as well as the trigonometric parallax distance, $d_\pi = 2755 \pm 326$ pc, estimated in this study. For a more accurate comparison with literature studies, we converted this value to the *UBV*-based colour excess $E(B - V)$. We utilised the equation $E(G_{\text{BP}} - G_{\text{RP}}) = 1.41 \times E(B - V)$ given by Sun et al. (2021) and determined the value as $E(B - V) = 0.301 \pm 0.033$ mag. This result is close to the values given by Tadross (2001), Lata et al. (2002), Carraro & Costa (2007) and Hasegawa et al. (2008) within the errors (see Table 1).

We also estimated heliocentric Galactic coordinates $(X, Y, Z)_\odot$ of Coll 74. Here, X is the distance from the Galactic center in the Galactic plane ($l = 0^\circ, b = 0^\circ$), Y is the distance in the direction of Galactic rotation ($l = 90^\circ, b = 0^\circ$) and Z is the vertical distance from Galactic plane to the North Galactic Pole ($l = 0^\circ, b = 90^\circ$). Galactocentric coordinates provide a convenient way to describe the positions of celestial objects relative to the Galactic center, Sun, and Galactic plane. By considering isochrone distance, Galactic longitude, and latitude of the cluster, we derived these distances as $(X, Y, Z)_\odot = (-2633, -907, -510)$ pc.

¹ <https://github.com/jobovy/isodist/blob/master/isodist/Isochrone.py>

4. GALACTIC ORBIT STUDY OF THE COLLINDER 74

The Galactic orbits of open clusters are important for understanding how these celestial objects dynamically evolve within the Milky Way (Taşdemir & Yontan 2023). We derived the orbits and orbital parameters of Coll 74 with the help of the python based Galactic dynamics library GALPY² of Bovy (2015). This library implements MWPOTENTIAL2014 model, which commonly uses a potential model in Galactic dynamics. The MWPOTENTIAL2014 model is based on a combination of different components that represent the various structures within the Milky Way, including the bulge, disc, and halo. These components are parameterised to approximate the observed properties of the Galaxy: the bulge is modelled as a power-law density profile as described in Bovy (2015), the disc is typically modelled as an exponential disk with a specified scale length and scale height as defined by Miyamoto & Nagai (1975) and the halo is often modelled as a spherical or ellipsoidal distribution with a specified density profile as defined by Navarro et al. (1996). We accepted Sun's Galactocentric distance and orbital velocity as $R_{gc} = 8$ kpc and $V_{rot} = 220$ km s⁻¹, respectively (Bovy 2015; Bovy & Tremaine 2012), as well as Sun's distance from the Galactic plane was adopted as 25 ± 5 pc (Jurić et al. 2008).

The mean radial velocity (V_γ) of the cluster was calculated from available *Gaia* DR3 radial velocity measurements of the stars. We considered the most likely member stars with probabilities over $P \geq 0.5$ whose number are 16. We used the equations of Soubiran et al. (2018) which are based on the weighted average of the radial velocities of the stars. Hence, the mean radial velocity of the Coll 74 was determined as $V_\gamma = 20.55 \pm 0.41$ km s⁻¹ which is in good agreement with mean radial velocity findings presented by Soubiran et al. (2018), Dias et al. (2021), Tarricq et al. (2021) and Hunt & Reffert (2023). To estimate orbital parameters, we used equatorial coordinates ($\alpha = 05^h48^m40^s.8$, $\delta = +07^\circ22'26''.4$) taken from Cantat-Gaudin et al. (2020), mean proper-motion components ($\mu_\alpha \cos \delta = 0.960 \pm 0.005$, $\mu_\delta = -1.526 \pm 0.004$ mas yr⁻¹), isochrone distance ($d_{iso} = 2831 \pm 118$ pc) and the radial velocity ($V_\gamma = 20.55 \pm 0.41$ km s⁻¹) calculated in the study (see also Table 2) for Coll 74 as input parameters.

The orbit integration was applied for the forward with an integration step of 1 Myr up to 2.5 Gyr to estimate the possible current position of Coll 74. The resultant orbit is shown in Figure 8a. The figure pictures the path followed by the cluster in $Z \times R_{gc}$ plane, which represents the side view of the orbit. Here, Z and R_{gc} are the distance from the Galactic plane and the Galactic center, respectively. Also, the orbit analyses were carried out for the past epoch across a time equal to $t = 1800 \pm 200$ Myr of the cluster's age. Figure 8b shows the cluster's distance variation in time on the $R_{gc} \times t$ plane. The figure also

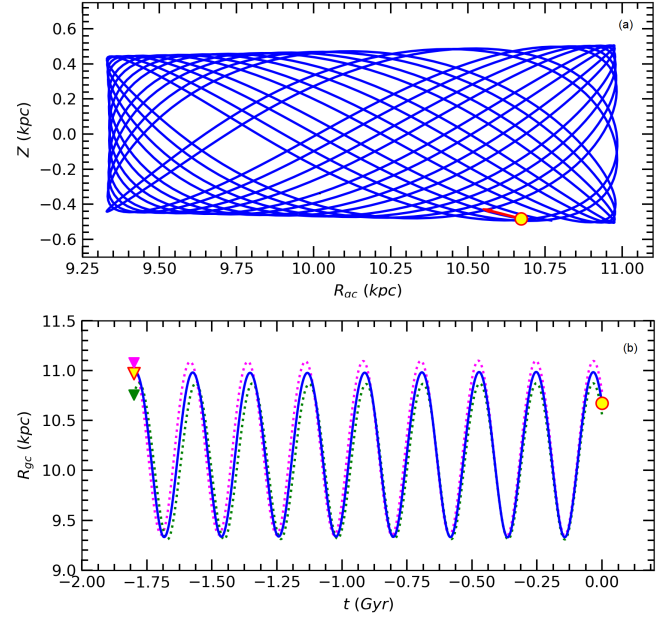


Figure 8. The Galactic orbits and birth radii of Coll 74 in the $Z \times R_{gc}$ (a) and $R_{gc} \times t$ (b) planes. The filled yellow circles and triangles show the present-day and birth positions, respectively. The red arrow is the motion vector of Coll 74. The green and pink dotted lines show the orbit when errors in input parameters are considered, while the green and pink filled triangles represent the birth locations of the open cluster based on the lower and upper error estimates.

represents the influence of errors in the input parameters on the orbit of Coll 74. Orbit analyses stated that the Coll 74 was formed outside the solar vicinity with a birth radius of $R_{gc} = 10.97 \pm 0.32$ kpc.

From the orbit integration we derived the following parameters for Coll 74: apogalactic ($R_a = 10987 \pm 112$ pc) and perigalactic ($R_p = 9337 \pm 20$ pc) distances, eccentricity ($e = 0.081 \pm 0.004$), maximum vertical distance from Galactic plane ($Z_{max} = 506 \pm 22$ pc), space velocity components ($U, V, W = -11.43 \pm 0.79, -29.50 \pm 1.08, -2.56 \pm 0.05$ km s⁻¹), and orbital period ($P_{orb} = 291 \pm 2$ Myr). The Local Standard of Rest (LSR) correction was applied to the (U, V, W) components of the Coll 74. To do this, we considered the space velocity component values (U, V, W)_⊙ = (8.83 ± 0.24, 14.19 ± 0.34, 6.57 ± 0.21) km s⁻¹ of Coşkunoğlu et al. (2011). Hence, LSR corrected space velocity components were found to be (U, V, W)_{LSR} = (-2.60 ± 0.25, -15.31 ± 1.13, 4.01 ± 0.22) km s⁻¹. Total space velocity was estimated as $S_{LSR} = 16.04 \pm 1.18$ km s⁻¹, which is compatible with the velocity value given for thin-disc objects (Leggett 1992). We interpreted from the perigalactic and apogalactic distances that Coll 74 is completely outside the solar circle (Figure 8a). The cluster reaches a maximum distance above the Galactic plane at $Z_{max} = 506 \pm 22$ pc, which shows that Coll 74 belongs to the thin-disc component of the Milky Way (Bilir et al. 2006a,b, 2008).

² See also <https://galpy.readthedocs.io/en/v1.5.0/>

5. LUMINOSITY AND MASS FUNCTIONS

The luminosity function (LF) of an open cluster represents the number of stars at different brightness within the cluster. The LF and mass function (MF) of open clusters are related because the luminosity of a star is generally correlated with its mass. This correlation is also defined as mass-luminosity relation and provides transformation of LF into the MF (Bisht et al. 2019).

For LF analyses of Coll 74, first, we selected the main-sequence stars with membership probabilities $P > 0$ and located inside the limiting radius obtained in the study ($r_{\text{lim}}^{\text{obs}} = 10'$). Hence, we reached 324 stars within the $15 \leq G \leq 20.5$ magnitude interval. Then considering distance modulus ($M_G = G - 5 \times \log d + A_G$) with apparent magnitude (G), isochrone distance (d_{iso}) and G band absorption (A_G) estimated in the study, we transformed apparent G magnitudes into the absolute M_G magnitudes. The histogram of LF for the cluster that constructed an interval of 1 mag is shown in Figure 9. This figure shows that the number of main-sequence stars increases up to $M_G=6$ mag properly, after this limit the counts drop gradually.

For MF estimation, we used PARSEC isochrones (Bressan et al. 2012) that scaled to the derived age and adopted metallicity fraction (z) for the cluster. From this isochrone, we produced a high-degree polynomial equation between the G -band absolute magnitudes and masses. By applying this equation to the selected main-sequence stars ($P > 0$), we transformed their absolute magnitudes M_G into masses. Hence, we found a mass range of the 324 stars within the $0.65 \leq M/M_{\odot} \leq 1.58$. The MF slope was derived from the following equation:

$$\log(dN/dM) = -(1 + \Gamma) \times \log M + C. \quad (4)$$

In the equation dN is the number of stars per unit mass dM , M is the central mass, C denotes the constant for the equation, and Γ represents the slope of the MF. The estimated MF slope for Coll 74 is $\Gamma = 1.34 \pm 0.21$, which is in good agreement with the value of Salpeter (1955). The resulting MF is shown in Figure 10.

The masses of stars in Coll 74 were derived as a function of stars' membership probabilities. The number of stars with probabilities $P > 0$ and $P \geq 0.5$ was determined as 324 and

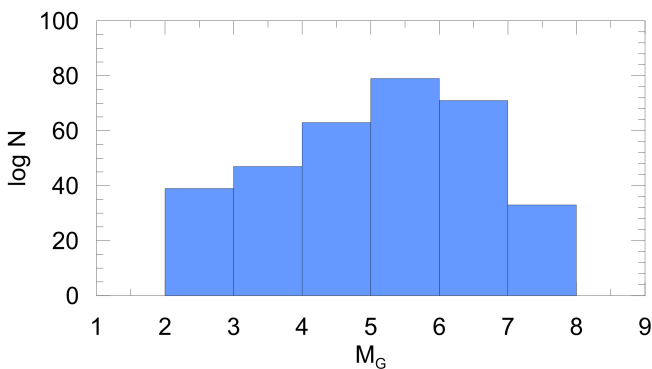


Figure 9. The luminosity function of Coll 74.

102, respectively. Hence, the total mass of the cluster for these probabilities is to be $365M_{\odot}$ and $132M_{\odot}$, respectively. We interpreted that the total mass of the cluster estimated from the stars with probabilities $P \geq 0.5$ corresponds to about 36% of the total mass for the stars with all probabilities. To investigate the mass distribution of the stars in Coll 74, 324 stars with $P > 0$ were plotted according to their equatorial coordinates and membership probabilities as shown in Figure 11. It can be interpreted from the figure that the stars with probabilities over 0.8 and massive ones are mostly concentrated central region of the cluster, whereas low-mass stars with probabilities under 0.8 are distributed beyond the cluster center. This case shows that the Coll 74 is a mass segregated open cluster.

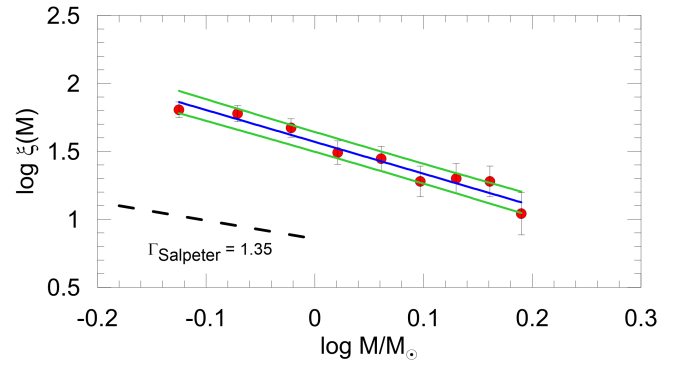


Figure 10. Derived mass function for Coll 74. The blue line represents the MF, whereas the green lines indicate the $\pm 1\sigma$ standard deviations. The black dashed line represented Salpeter (1955)'s slope.

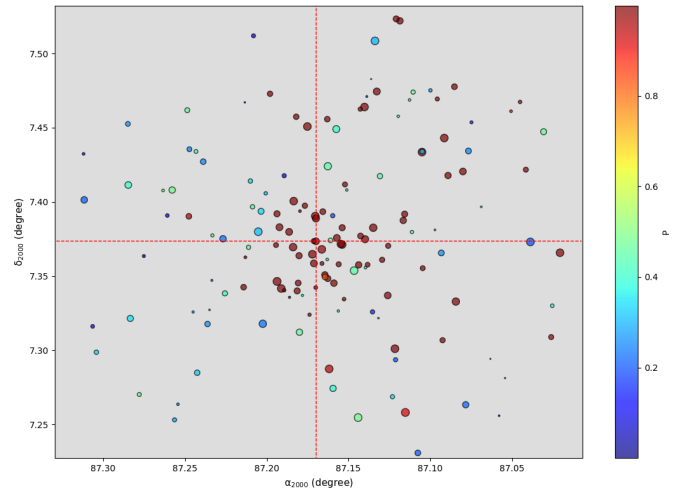


Figure 11. Mass distribution of the stars in the Coll 74. The radius sizes of the stars indicate the masses, and the different colours show the membership probabilities of the stars. The intersection of the red dashed lines indicates the central position of the cluster in the equatorial coordinate system.

6. CONCLUSION

We performed a detailed *Gaia* DR3 data-based study of open cluster Collinder 74. The number of member stars with prob-

abilities over 0.5 were 102. Considering these stars, we calculated structural and fundamental astrophysical parameters, investigated luminosity and mass functions, and estimated the orbit of the cluster. All parameters obtained in the study are listed in Table 2. The main results of the study are summarized as follows:

1. From the RDP analyses, we determined the limiting radius by visual inspection as $r_{\text{lim}}^{\text{obs}} = 10'$.

2. Considering results of photometric completeness limit, membership probability analyses, and limiting radius, we identified 102 most likely members with probabilities $P \geq 0.5$ for Coll 74. These stars were used in the cluster analyses.

3. The mean proper-motion components were obtained as $(\mu_{\alpha} \cos \delta, \mu_{\delta}) = (0.960 \pm 0.005, -1.526 \pm 0.004)$ mas yr⁻¹.

4. Four most probable BSS members were identified within the limiting radius of the cluster. We concluded that the Coll 74 belongs to family I according to the radial distribution of its BSSs.

5. The metallicity value for the cluster was adopted as $[\text{Fe}/\text{H}] = -0.052 \pm 0.034$ dex which is presented by [Zhong et al. \(2020\)](#). We transformed this value into the mass fraction $z = 0.0136$ and kept it as a constant parameter for the age and distance modulus estimation.

6. By fitting PARSEC isochrone ([Bressan et al. 2012](#)) to the G versus $(G_{\text{BP}} - G_{\text{RP}})$ colour-magnitude diagram, we estimated colour excess of the Coll 74 as $E(G_{\text{BP}} - G_{\text{RP}}) = 0.425 \pm 0.046$ mag, which corresponds to a colour excess in UBV system to be $E(B - V) = 0.301 \pm 0.033$ mag. We estimated this value by using the equation $E(G_{\text{BP}} - G_{\text{RP}}) = 1.41 \times E(B - V)$ as given by [Sun et al. \(2021\)](#).

7. The isochrone fitting distance of Coll 74 was determined as $d_{\text{iso}} = 2831 \pm 118$ pc. This value is supported by the distance $d_{\varpi} = 2755 \pm 326$ pc that derived from mean trigonometric parallax.

8. PARSEC isochrone of [Bressan et al. \(2012\)](#) provides the age of the cluster to be $t = 1800 \pm 200$ Myr.

9. The LF and MF were investigated from the main-sequence stars with probabilities $P > 0$. The MF slope was found as $\Gamma = 1.34 \pm 0.21$ which is in good agreement with the value of [Salpeter \(1955\)](#).

10. Orbit integration was performed via MWPOTENTIAL2014 model. We concluded that Coll 74 orbits in a boxy pattern outside the solar circle, as well as the cluster, is a member of the thin-disc component of the Milky Way. Moreover, the birth radius (10.97 ± 0.32 kpc) shows that the forming region of the cluster is outside the solar circle.

Peer Review: Externally peer-reviewed.

Author Contribution: Conception/Design of study - T.Y., R.C.; Data Acquisition - T.Y., R.C.; Data Analysis/Interpretation - T.Y., R.C.; Drafting Manuscript - T.Y.,

Table 2. Fundamental parameters of Coll 74.

Parameter	Value
$(\alpha, \delta)_{\text{J2000}}$ (Sexagesimal)	05:48:40.8, +07:22:26.4
$(l, b)_{\text{J2000}}$ (Decimal)	199.0189, -10.3791
f_0 (stars arcmin ⁻²)	8.42 ± 0.35
f_{bg} (stars arcmin ⁻²)	5.45 ± 0.16
r_c (arcmin)	1.38 ± 0.12
r_{lim} (arcmin)	10
r (pc)	8.24
Cluster members ($P \geq 0.5$)	102
$\mu_{\alpha} \cos \delta$ (mas yr ⁻¹)	0.960 ± 0.005
μ_{δ} (mas yr ⁻¹)	-1.526 ± 0.004
ϖ (mas)	0.363 ± 0.043
d_{ϖ} (pc)	2755 ± 326
$E(B - V)$ (mag)	0.301 ± 0.033
$E(G_{\text{BP}} - G_{\text{RP}})$ (mag)	0.425 ± 0.046
A_G (mag)	0.792 ± 0.086
$[\text{Fe}/\text{H}]$ (dex)*	-0.052 ± 0.034
Age (Myr)	1800 ± 200
Distance modulus (mag)	13.052 ± 0.088
Isochrone distance (pc)	2831 ± 118
$(X, Y, Z)_{\odot}$ (pc)	$(-2633, -907, -510)$
R_{gc} (kpc)	10.67
MF slope	1.34 ± 0.21
Total mass (M/M_{\odot}) ($P > 0$)	365
V_{γ} (km s ⁻¹)	20.55 ± 0.41
U_{LSR} (km s ⁻¹)	-2.60 ± 0.25
V_{LSR} (kms ⁻¹)	-15.31 ± 1.13
W_{LSR} (kms ⁻¹)	4.01 ± 0.22
S_{LSR} (kms ⁻¹)	16.04 ± 1.18
R_a (pc)	10987 ± 112
R_p (pc)	9337 ± 20
z_{max} (pc)	506 ± 22
e	0.081 ± 0.004
P_{orb} (Myr)	291 ± 2
Birthplace (kpc)	10.97 ± 0.32

*[Zhong et al. \(2020\)](#)

R.C.; Critical Revision of Manuscript - T.Y., R.C.; Final Approval and Accountability - T.Y., R.C.

Conflict of Interest: Authors declared no conflict of interest.

Financial Disclosure: This study has been supported in part by the Scientific and Technological Research Council (TÜBİTAK) 122F109

Acknowledgements: This research has made use of the WEBDA database, operated at the Department of Theoretical Physics and Astrophysics of the Masaryk University. We also made use of NASA's Astrophysics Data System as well as

the VizieR and Simbad databases at CDS, Strasbourg, France and data from the European Space Agency (ESA) mission *Gaia*³, processed by the *Gaia* Data Processing and Analysis Consortium (DPAC)⁴. Funding for DPAC has been provided by national institutions, in particular, the institutions participating in the *Gaia* Multilateral Agreement.

LIST OF AUTHOR ORCIDS

T. Yontan <https://orcid.org/0000-0002-5657-6194>

R. Canbay <https://orcid.org/0000-0003-2575-9892>

REFERENCES

- Ann H. B., Lee M. G., Chun M. Y., Kim S. L., Jeon Y. B., Park B. G., 1999, *Journal of Korean Astronomical Society*, 32, 7
- Bilir S., Karaali S., Ak S., Yaz E., Hamzaoglu E., 2006a, *New Astron.*, 12, 234
- Bilir S., Karaali S., Gilmore G., 2006b, *MNRAS*, 366, 1295
- Bilir S., Cabrera-Lavers A., Karaali S., Ak S., Yaz E., López-Corredoira M., 2008, *Publ. Astron. Soc. Australia*, 25, 69
- Bisht D., Yadav R. K. S., Ganesh S., Durgapal A. K., Rangwal G., Fynbo J. P. U., 2019, *MNRAS*, 482, 1471
- Bisht D., Zhu Q., Yadav R. K. S., Durgapal A., Rangwal G., 2020, *MNRAS*, 494, 607
- Bovy J., 2015, *ApJS*, 216, 29
- Bovy J., Tremaine S., 2012, *ApJ*, 756, 89
- Bressan A., Marigo P., Girardi L., Salasnich B., Dal Cero C., Rubele S., Nanni A., 2012, *MNRAS*, 427, 127
- Cantat-Gaudin T., et al., 2018, *A&A*, 618, A93
- Cantat-Gaudin T., et al., 2020, *A&A*, 640, A1
- Carraro G., Costa E., 2007, *A&A*, 464, 573
- Carraro G., Sales Silva J. V., Moni Bidin C., Vazquez R. A., 2017, *AJ*, 153, 99
- Coşkunoğlu B., et al., 2011, *MNRAS*, 412, 1237
- Dias W. S., Assafin M., Flório V., Alessi B. S., Lîbero V., 2006, *A&A*, 446, 949
- Dias W. S., Monteiro H., Caetano T. C., Lépine J. R. D., Assafin M., Oliveira A. F., 2014, *A&A*, 564, A79
- Dias W. S., Monteiro H., Assafin M., 2018, *MNRAS*, 478, 5184
- Dias W. S., Monteir H., Moitinho A., Lépine J. R. D., Carraro G., Paunzen E., Alessi B., Villela L., 2021, *MNRAS*, 504, 356
- Ferraro F. R., et al., 2012, *Nature*, 492, 393
- Gaia Collaboration et al., 2016, *A&A*, 595, A1
- Gaia Collaboration et al., 2018, *A&A*, 616, A1
- Gaia Collaboration et al., 2023, *A&A*, 674, A1
- Hasegawa T., Sakamoto T., Malasan H. L., 2008, *PASJ*, 60, 1267
- Hills J. G., Day C. A., 1976, *Astrophys. Lett.*, 17, 87
- Hunt E. L., Reffert S., 2023, *A&A*, 673, A114
- Jadhav V. V., Subramaniam A., 2021, *MNRAS*, 507, 1699
- Jurić M., et al., 2008, *ApJ*, 673, 864
- Kharchenko N. V., Piskunov A. E., Schilbach E., Röser S., Scholz R. D., 2013, *A&A*, 558, A53
- Kim S. C., Kyeong J., Park H. S., Han I., Lee J. H., Moon D.-S., Lee Y., Kim S., 2017, *Journal of Korean Astronomical Society*, 50, 79
- King I., 1962, *AJ*, 67, 471
- Krone-Martins A., Moitinho A., 2014, *A&A*, 561, A57
- Lada C. J., Lada E. A., 2003, *ARA&A*, 41, 57
- Lata S., Pandey A. K., Sagar R., Mohan V., 2002, *A&A*, 388, 158
- Leggett S. K., 1992, *ApJS*, 82, 351
- Liu L., Pang X., 2019, *ApJS*, 245, 32
- Loktin A. V., Popova M. E., 2017, *Astrophysical Bulletin*, 72, 257
- Marsakov V. A., Gozha M. L., Koval' V. V., Shpigel' L. V., 2016, *Astronomy Reports*, 60, 43
- Miyamoto M., Nagai R., 1975, *PASJ*, 27, 533
- Navarro J. F., Frenk C. S., White S. D. M., 1996, *ApJ*, 462, 563
- Rain M. J., Ahumada J. A., Carraro G., 2021, *A&A*, 650, A67
- Salpeter E. E., 1955, *ApJ*, 121, 161
- Sandage A. R., 1953, *AJ*, 58, 61
- Sariya D. P., et al., 2021, *AJ*, 161, 101
- Soubiran C., et al., 2018, *A&A*, 619, A155
- Sun M., Jiang B., Yuan H., Li J., 2021, *ApJS*, 254, 38
- Taşdemir S., Yontan T., 2023, *Physics and Astronomy Reports*, 1, 1
- Tadross A. L., 2001, *New Astron.*, 6, 293
- Tarricq Y., et al., 2021, *A&A*, 647, A19
- Zacharias N., Finch C. T., Girard T. M., Henden A., Bartlett J. L., Monet D. G., Zacharias M. I., 2013, *AJ*, 145, 44
- Zhong J., Chen L., Wu D., Li L., Bai L., Hou J., 2020, *A&A*, 640, A127
- Zinn R., Dahn C. C., 1976, *AJ*, 81, 527

³ <https://www.cosmos.esa.int/gaia>

⁴ <https://www.cosmos.esa.int/web/gaia/dpac/consortium>